

## Highlights

### **Reducing RES Droughts through the integration of wind and solar PV**

Boris Morin, Aina Maimó Far, Damian Flynn, Conor Sweeney

- RES droughts are analysed using 45 years of hourly wind and solar PV generation data
- RES droughts from C3S-Energy and ERA5-Atlite datasets are compared
- Adding solar PV to a wind-dominated system reduces RES drought frequency and duration
- Validated RES datasets are crucial to accurately identify RES drought extremes

# Reducing RES Droughts through the integration of wind and solar PV

Boris Morin<sup>a,\*</sup>, Aina Maimó Far<sup>a</sup>, Damian Flynn<sup>b</sup>, Conor Sweeney<sup>a</sup>

*<sup>a</sup>School of Mathematics and Statistics, University College Dublin, Belfield, Dublin  
4, Dublin, D04 V1W8, Ireland*

*<sup>b</sup>School of Electrical and Electronic Engineering, University College Dublin, Belfield,  
Dublin 4, Dublin, D04 V1W8, Ireland*

---

\*Corresponding author

*Email addresses:* `boris.morin@ucdconnect.ie` (Boris Morin ),  
`aina.maimofar@ucd.ie` (Aina Maimó Far), `damian.flynn@ucd.ie` (Damian Flynn),  
`conor.sweeney@ucd.ie` (Conor Sweeney)

---

## Abstract

Increasing the share of electricity produced from renewable energy sources (RES), combined with RES dependence on weather, poses a critical challenge for energy systems. This study investigates the importance of the balance between wind and solar photovoltaic (PV) capacity on periods of low renewable generation, known as RES droughts. Three different RES datasets are used to estimate the capacity factors for different scenarios of installed capacities for wind and solar PV power. The skill of the RES models is quantified by comparing capacity factor time series to observed hourly data and by assessing their representation of observed RES droughts. The RES models are used to generate a 45-year hourly time series of RES capacity factor, enabling analysis of the frequency, duration and return periods of RES droughts at a climatological scale. Results show the importance of using an accurate, validated RES model for RES drought risk assessment. The addition of solar PV capacity to a wind-dominated system results in a significant reduction in the frequency and duration of RES droughts, while also reducing extremes and seasonal RES drought patterns. These findings underscore the importance of diversification in RES capacity to enhance energy security and resilience.

*Keywords:* RES Drought, Wind Power, Solar PV Power, Renewable Energy Sources, Return Periods

---

## 1. Introduction

The EU aims to generate at least 69% of its electricity from renewable energy sources (RES) by 2030, up from 41% in 2022 [1]. While this transition is essential for reducing greenhouse gas emissions, it also highlights the challenge of managing the variability of weather-dependent energy sources such as wind and solar photovoltaic (PV) power. This challenge is amplified by the increasing electrification of energy sectors, which places greater demand on the power system and makes it more sensitive to meteorological conditions, both in historical [2] and future climates [3]. Periods of low renewable generation, known as *Dunkelflaute* or RES droughts, pose significant risks to system adequacy and energy security, emphasising the need for a resilient energy system to meet both growing electricity demand and decarbonisation targets.

RES drought events do not have a fixed definition, with various approaches present in the literature. One common method defines a RES drought as a period during which the average capacity factor (CF) remains below a fixed threshold for a specified duration. For example, Kaspar et al. [4] used this method to investigate the shortfall risks of low wind and solar PV generation in Europe, with a focus on Germany, testing multiple CF thresholds and durations. Similarly, Mockert et al. [5] examined the link between weather regimes and RES droughts in Germany using a 48-hour rolling window under a threshold to define RES droughts. Similar fixed-threshold approaches have also been applied using CF series reconstructed through machine learning in regions such as Japan [6] and Hungary [7].

Alternative methods adjust the CF threshold dynamically over the year to account for seasonal variations in renewable production. Raynaud et al. [8] defined RES droughts as sequences of days with renewable electricity generation below a threshold that varies seasonally, a methodology later adapted for India [9]. Building on this, Kapica et al. [10] compared the likelihood of increased RES droughts in Europe under different climate models. Other studies have defined RES droughts based on deviations from daily mean production: Rinaldi et al. [11] applied these in the U.S. Western Interconnection to quantify the benefits of long-term storage, while Brown et al. [12] examined weekly timescales to explore meteorological influences on the most severe RES drought events. Another method defines RES drought indices based on metrics commonly used in hydro-meteorology to characterise RES droughts [13]. This approach identifies periods of unusually low generation relative to historical production levels, using the lowest production percentiles. Bracken et al. [14] used this approach to analyse RES droughts at different time scales in the U.S. [14], and Lei et al. [15] used it to quantify RES droughts in wind-PV-hydro systems in China.

In addition to examining periods of low renewable electricity generation, several studies also explore the periods when the imbalance between renewable generation and electricity demand (residual demand) is high. Raynaud et al. [8] showed the difference between RES droughts and high residual demand events in a hypothetical fully renewable system composed of wind, solar PV and run-of-the-river hydropower. Similarly, Allen and Otero [13] also defined a standardised index based on meteorological droughts to address residual demand, whose correlation to the electricity generation index is mostly negative (as expected, although quite low anticorrelations and even small positive correlations appear for some European countries). This index

was also applied to the U.S. by Bracken et al. [14], revealing a consistent increase in the RES drought magnitude when demand is considered, despite showing differing results across regions.

In this paper, the focus is exclusively on renewable electricity generation, to keep the focus on RES droughts driven by the weather. A fixed threshold approach is used to define RES droughts, which facilitates consistent inter-comparison between scenarios with different installed wind and solar PV capacities. The case study used in this paper is Ireland, a region where most RES generation comes from wind power and with ambitious targets for solar PV power expansion. This provides valuable insights into the potential benefits of adding solar PV installations in wind-dominated countries.

RES droughts are identified using onshore wind and solar PV CF time series. In this study, three different datasets are used and compared, all of which are driven by the ERA5 reanalysis [16]. Two of the datasets are part of C3S Energy (C3SE), an energy-based operational dataset produced by the EU Copernicus Climate Change Service [17]. One of the C3SE datasets provides CF time series aggregated at the national scale, while the other provides the CF time series at each grid point, at the ERA5 resolution of  $0.25^\circ$ . The third dataset produced by the authors was generated using the Atlite model [18], which converts the ERA5 atmospheric data to a generation time series using specified wind turbine and PV panel models. Atlite is an open-source tool developed by PyPSA [18] and has been used for estimating wind and solar PV generation in order to study RES droughts in Germany [5].

Generic datasets for wind and solar PV CF are often used for the quantification of RES droughts. Despite undergoing a validation process, they are often not fully representative of each geographical location, and can show differences in the number of RES drought events [19]. This study evaluates the skill of a dataset developed for the European region (C3SE) when applied to a specific country (Ireland). In particular, the analysis explores the impact of using a generic versus a tailored dataset on RES drought assessments, in the context of a transition from a wind-dominated system to one with a greater share of solar PV.

The aim of this study is to answer two questions which are relevant for systems with a large share of RES generation:

- Do generic datasets have sufficient skill to reliably quantify RES drought events?
- How does the integration of solar PV into a predominantly wind-based

89 system alter the characteristics of RES drought events?

90 The datasets used in this study are detailed in section 2, which describes  
91 their characteristics and relevance for evaluating RES droughts. Section 3  
92 outlines the RES datasets used to simulate wind and solar PV generation and  
93 provides the methodology for defining and identifying RES drought events,  
94 including the thresholds and metrics applied. In section 4, the datasets are  
95 first verified against observed energy data to assess their accuracy, followed by  
96 an analysis of RES drought occurrences for two scenarios with different ratios  
97 of installed wind to solar PV capacities. Finally, section 5 offers a discussion  
98 of the results in the context of energy reliability and future planning, followed  
99 by the main conclusions and recommendations for further research.

## 100 2. Data

101 This study uses publicly available datasets to construct and validate the  
102 datasets for estimating the CF of wind and solar PV power. The primary  
103 data sources include: EirGrid and SONI, the transmission system operators  
104 (TSO) for the Republic of Ireland and Northern Ireland, respectively; the  
105 ERA5 reanalysis dataset; and the C3SE dataset.

### 106 2.1. Wind and solar PV Capacity and Availability

107 EirGrid, the TSO for the Republic of Ireland, and SONI, the Northern  
108 Ireland TSO, provide detailed datasets on all wind and solar PV farms across  
109 the island of Ireland (Republic of Ireland and Northern Ireland) from 1990  
110 to the present [20]. These datasets include information such as each farm’s  
111 installed capacity, name, and connection date. To enhance the accuracy of  
112 this data, the longitude and latitude for each farm were manually determined  
113 through online searches. For simplicity, this data will be referred to as orig-  
114 inating from EirGrid, as all-island data was directly obtained from EirGrid,  
115 and the combined regions of the Republic of Ireland and Northern Ireland  
116 will be referred to as Ireland throughout the remainder of this document.

117 The spreadsheet available from the EirGrid website contains two key vari-  
118 ables: generation and availability. Generation is the energy that a RES farm  
119 actually contributed to the grid, which may include limitations introduced  
120 by the TSO to maintain grid stability, such as constraints and curtailment.  
121 Availability represents the energy that would have been generated from a RES  
122 farm if no grid constraints had been applied, making it representative of the

123 weather-related response. Generation and availability values are available  
 124 from 2014 onward for wind power and from 2018 onward for solar PV power,  
 125 although solar PV availability data only became present in the Republic of  
 126 Ireland in 2023. This study focuses on availability for all analyses.

## 127 2.2. Atmospheric Variables

128 All of the datasets used in this study are driven by data from the ERA5 re-  
 129 analysis [16], produced by the European Centre for Medium-Range Weather  
 130 Forecasts (ECMWF). This global gridded dataset provides hourly atmo-  
 131 spheric variables from 1940 to the present at a horizontal resolution of  $0.25^\circ$ .  
 132 Table 1 lists the relevant ERA5 variables.

Table 1: ERA5 variables used to calculate wind and solar PV generation

ERA5 name	variable
100 metre zonal and meridional wind speed	$u_{100}, v_{100}$
2 metre temperature	$t2m$
Surface net solar radiation	$ssr$
Surface solar radiation downwards	$ssrd$
Top of atmosphere incident radiation	$tisr$
Total sky direct solar radiation at surface	$fdir$

## 133 2.3. C3S Energy

134 The EU Copernicus Climate Change Service developed the C3S-Energy  
 135 (C3SE) renewable energy dataset for Europe [17], using ERA5 atmospheric  
 136 variables and weather-to-energy models. This dataset provides hourly CF for  
 137 wind and solar PV power from 1979 to the present. The data are available  
 138 on the same grid as the ERA5 data, which has a horizontal resolution of  
 139  $0.25^\circ$ . The time series are also available for download at two aggregated  
 140 scales: regional (NUTS 2) and national.

141 The wind CF in C3SE was calculated using wind speeds at 100 metres  
 142 ( $u_{100}, v_{100}$ ) and a standard turbine model, the Vestas V136/3450, with a fixed  
 143 hub height of 100 meters. As data on wind turbine fleet locations and speci-  
 144 fications are difficult to obtain across Europe, C3SE assumes a homogeneous  
 145 distribution of wind turbines across the ERA5 grid. While this approach  
 146 does not capture the precise capacity factors reported by grid operators, it  
 147 provides a well-correlated time series that effectively represents the impact

of climate variability on wind power generation. The C3SE solar PV CF was also calculated for the ERA5 grid. It is derived from meteorological data, including surface solar radiation downwards (*ssrd*) and air temperature (*t2m*), using a reference solar PV plant model. This model incorporates empirical calculations for key system components such as optical losses, module efficiency, and inverters. The final CF accounts for a mix of module orientations typical for each location [21].

### 3. Methods

This study analyses RES droughts across the island of Ireland using on-shore wind and solar PV CF time series from three datasets: two from C3SE, based on national-level data (C3S NAT) and grid-level data (C3S GRD), and one derived from the Atlite model (ATL).

#### 3.1. C3S Energy National: C3S NAT

The C3S NAT dataset is created by combining two inputs provided by C3SE at the corresponding NUTS levels: Republic of Ireland (NUTS0: IE) and Northern Ireland (NUTS2: UKN0). The two inputs are combined, using the actual installed capacity as weights. This dataset assumes that RES generation occurs at every ERA5 grid point in Ireland.

#### 3.2. C3S Energy Gridded: C3S GRD

The C3S GRD dataset uses, as inputs, the actual locations of the RES farms in Ireland, and the CF from C3SE over the ERA5 grid. For each farm, the CF from the nearest grid point on the C3SE dataset was selected. A weighted average of the CF associated with each farm, using the farm's installed capacities, was used to produce the total CF time series.

#### 3.3. Atlite: ATL

The ATL dataset is produced using the Atlite model. Atlite allows the user to define the wind turbine power curve and PV panel model to use when converting weather variables to wind and solar PV generation. The Atlite model takes as inputs the locations of RES farms and ERA5 weather variables: wind speed at 100 metres ( $u_{100}$ ,  $v_{100}$ ) for wind generation, and radiation variables (*ssr*, *ssrd*, *tisr*, and *fdir*) along with air temperature (*t2m*) for solar PV generation. The output of the Atlite model is a generation time series, which is divided by the total capacity to transform it back into



181 CF. The selection of the wind turbine power curve and PV panel model  
182 represents the key difference between this dataset and C3S GRD. This study  
183 identifies the most appropriate wind turbine power curve to use from the  
184 121 power curves, each at five different levels of smoothing, made available  
185 by Renewables.ninja [22], and selects the PV panel model out of the options  
186 available within Atlite.

### 187 3.4. Energy Scenarios

188 The three datasets provide CF time series for both wind and solar PV. In  
189 addition to analysing the CF of wind and solar PV separately, a combined  
190 CF was computed for each dataset by averaging wind and solar PV CF,  
191 weighted by their installed capacities at the end of 2023 (5.9 GW for wind  
192 power and 0.6 GW for solar PV power). This configuration is referred to as  
193 the 91W-9PV scenario, reflecting the distribution of 91% wind and 9% solar  
194 PV capacity. Given that solar PV capacity in Ireland is low in 2023, and to  
195 explore how a more balanced distribution of wind and solar PV capacities  
196 might impact RES droughts, this study also considered a second scenario,  
197 referred to as 57W-43PV, where the installed solar PV capacity is assumed  
198 to increase to 8.6 GW, while wind capacity rises to 11.45 GW. These values  
199 are based on targets outlined in the roadmap published by the 2024 Climate  
200 Action Plan [23]. This study does not include offshore wind in the analysis.  
201 Recent reports suggest that even by 2030, Ireland is unlikely to have any  
202 significant new offshore wind farms, with projected offshore capacity expected  
203 to remain near zero using realistic scenarios [24].

204 New time series were generated for both the ATL and C3S GRD solar  
205 PV datasets, incorporating a revised distribution of installed capacity across  
206 Ireland as specified in the roadmap. For wind power, the CF time series  
207 remains unchanged, as significant shifts in the location of wind farms are not  
208 expected. In total, twelve CF time series were analysed in this study, six for  
209 individual wind and solar PV CF (three datasets for each source) in the 91W-  
210 9PV scenario, and an additional six time series that include the combined  
211 CF for 91W-9PV and 57W-43PV scenarios across the different datasets.

212 It is important to note that the specific capacity values used in this study  
213 are illustrative and are not intended to reflect precise future realities. Instead,  
214 they serve to explore the impact of transitioning from a wind-dominated sys-  
215 tem (91W-9PV) to a more evenly distributed system (57W-43PV). This ap-  
216 proach allows for a comparative analysis between the two scenarios, assessing  
217 how the balance of RES capacity affects the occurrence of RES droughts.

218 For each dataset (ATL, C3S GRD, and C3S NAT), four distinct scenarios  
219 are examined, as summarised below:

- 220 • Wind Power - based on the actual capacity at the end of 2023
- 221 • Solar PV Power - based on the actual capacity at the end of 2023
- 222 • Combined RES / 91W-9PV - based on the actual capacity at the end  
223 of 2023
- 224 • Combined RES / 57W-43PV - based on the projected capacity for 2030

### 225 3.5. RES Drought Definition

226 In this study, a RES drought event was defined as occurring when the  
227 24-hour moving average of CF remains below a fixed threshold of 0.1 for a  
228 period of longer than 24 hours. By using a 24-hour moving average, fewer  
229 but longer-lasting events were captured compared to using the raw CF time  
230 series, which can be more sensitive to short-term fluctuations. The 24-hour  
231 rolling average also avoids potential masking of day-long events due to their  
232 start time. A fixed threshold approach was chosen in this study to enable  
233 consistent inter-comparison between datasets.

234 The moving average approach smooths out short-term fluctuations, so  
235 that brief periods above the threshold do not interrupt an otherwise continu-  
236 ous low-CF period (Fig. 1). This means that a single hour above the threshold  
237 does not "break" a RES drought event if it is surrounded by prolonged low-  
238 generation hours. As a result, fewer but longer-lasting RES drought events  
239 are identified, which may better reflect real-world conditions where energy  
240 supply constraints persist over extended periods.

## 241 4. Results

### 242 4.1. Verification

243 The accuracy of the datasets used in this study was verified, before con-  
244 tinuing to the analysis of RES droughts. For the verification process, time-  
245 varying values of installed capacity were used to account for changes in RES  
246 development over the verification period. This step allowed us to assess how  
247 well the datasets represent the production of renewable energy by compar-  
248 ing them against observed data. The general statistics of the observed data  
249 and the three datasets are presented in the violin plots in Fig. 2, considering

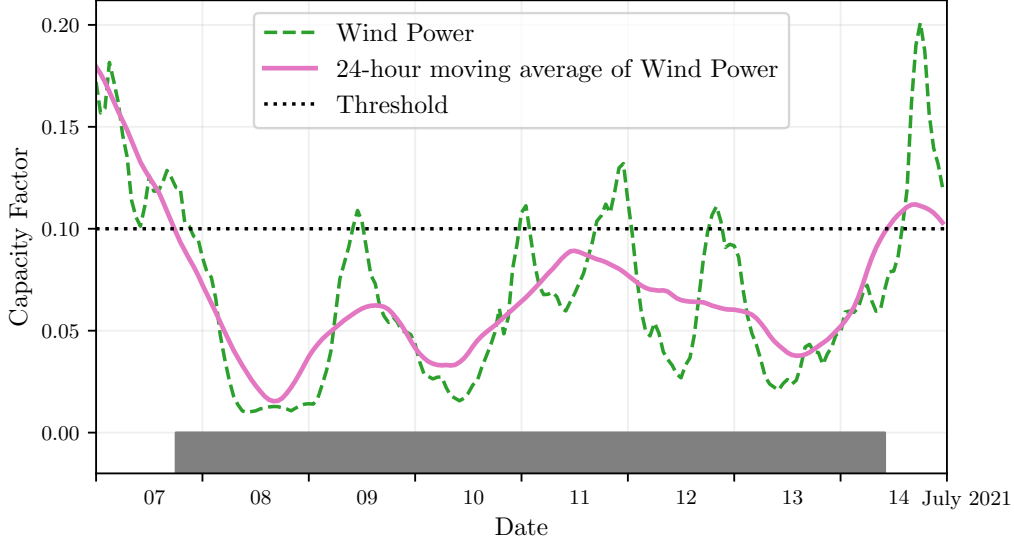


Figure 1: Wind time series of CF (green) and its 24-hour moving average (pink) from the 7th to the 15th of July 2021. The black dashed line indicates the CF threshold. The grey bar shows the period identified as a wind drought under our definition

the 2014-2023 validation period for wind and 2023 for solar PV. These plots illustrate the density of CF values for each dataset, highlighting differences between the datasets and their alignment with observed data. The general CF values show ATL aligns better with OBS for wind, and all datasets are similar for PV.

#### 4.1.1. Wind Energy

The C3S datasets use the Vestas V136/3450 wind turbine power curve (Fig. 3a). The Atlite model allows the user to specify the power curve. We considered the 121 power curves available for download from Renewables.ninja [22]. For each power curve, Renewables.ninja also provides four associated smoothed power curves. The smoothing is done using a Gaussian filter with different standard deviations that depend on the wind speed. A separate wind CF time series for Ireland was generated for each of the wind turbine power curves and smoothing levels.

The performance of each CF time series is then assessed based on four skill scores: correlation coefficient (CC), root mean square error (RMSE), mean bias error (MBE), and the percentage of overlap. The percentage of overlap

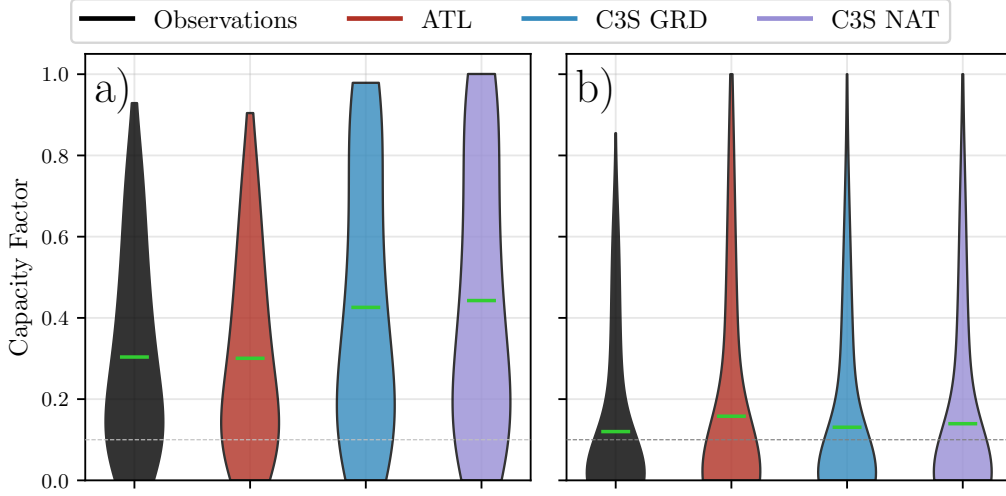


Figure 2: Violin plots of CF distributions for wind a) and solar PV b) datasets. Each violin represents the distribution of CF over time for different datasets: Observations (black), ATL (red), C3S GRD (blue), and C3S NAT (purple). The mean value for each dataset is marked with a green horizontal line. The red line indicates the threshold of 0.1 used in the study to identify RES droughts

quantifies the similarity between the observed and modelled distributions. It is a positively oriented skill score, where 100% shows full agreement between the two distributions, and 0% indicates no overlap. The histograms of hourly CF values for the most recent decade (2014-2023) are used to calculate this skill score.

Based on these metrics, the most representative power curve for Ireland is the Enercon E112.4500 power curve with the  $0.3w$  smoothing filter. The smoothing of the wind turbine power curve represents losses associated with each turbine, as well as losses such as wake effects between turbines, which are important when modelling wind energy on larger spatial scales. The histogram in Fig. 3b shows that the C3SE power curve tends to underestimate low CF values and overestimate higher ones, whereas the smoothed ATL power curve more closely follows the observed wind availability data. This is further supported by the percentage of overlap which is higher for ATL (97.2%) than for C3SE (83.2%), indicating better agreement with observed data.

The effect of the difference between the power curves is also visible in Fig. 4, which shows a density plot of wind CF values. The two C3S datasets

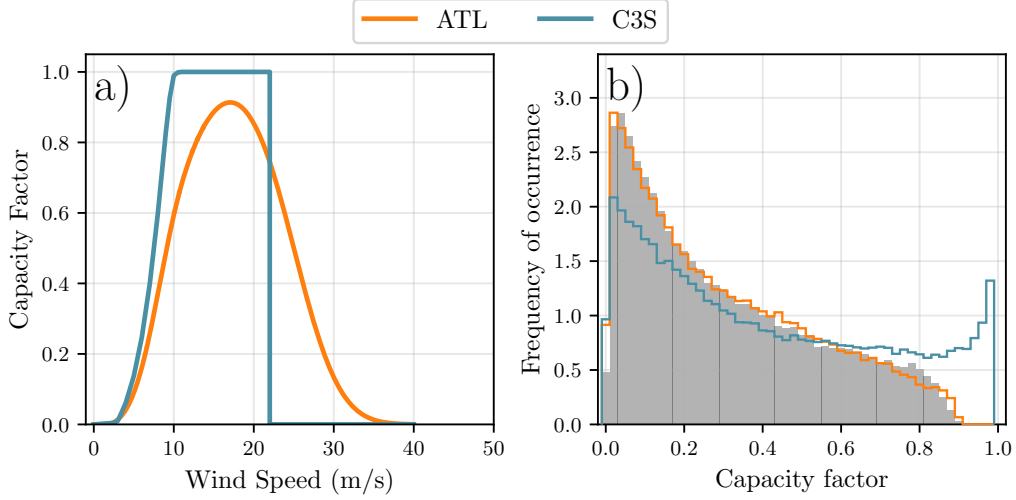


Figure 3: a) Power curves of the Enercon E112.4500 with a 0.3w smoothing filter used by ATL (orange) and the Vestas V136/3450 used by C3SE (blue) b) Histograms of wind CF for Ireland from ATL (orange), C3SE (blue) and Observed (shaded)

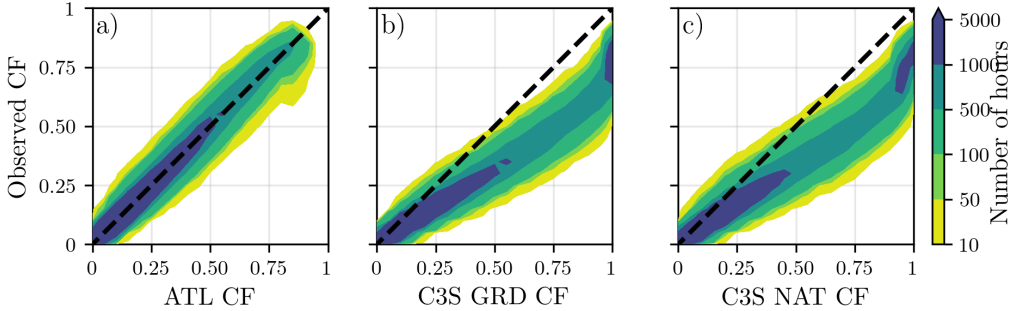


Figure 4: Wind CF density plot of the observed CF (vertical axes) and modelled (horizontal axes) CF data for the a) ATL, b) C3S GRD and c) C3S NAT datasets

are shown to overestimate the observed CF, whereas the ATL dataset is in good agreement with the observed data. The skill scores presented in Table 2 show that ATL performs better than the two C3S datasets for all of the skill scores.

Fig. 5 shows the average annual number of wind drought events during the 2014 to 2023 validation period. The figure reveals that ATL presents the best overall agreement with the observed frequency and duration of wind

	ATL	C3S GRD	C3S NAT
<b>CC</b>	0.981	0.972	0.970
<b>RMSE</b>	0.045	0.177	0.162
<b>MBE</b>	-0.003	0.137	0.121

Table 2: Skill scores for wind power for the three datasets compared to observed data

292 drought events. This pattern is particularly evident for shorter-duration  
293 events, which are the most frequent.

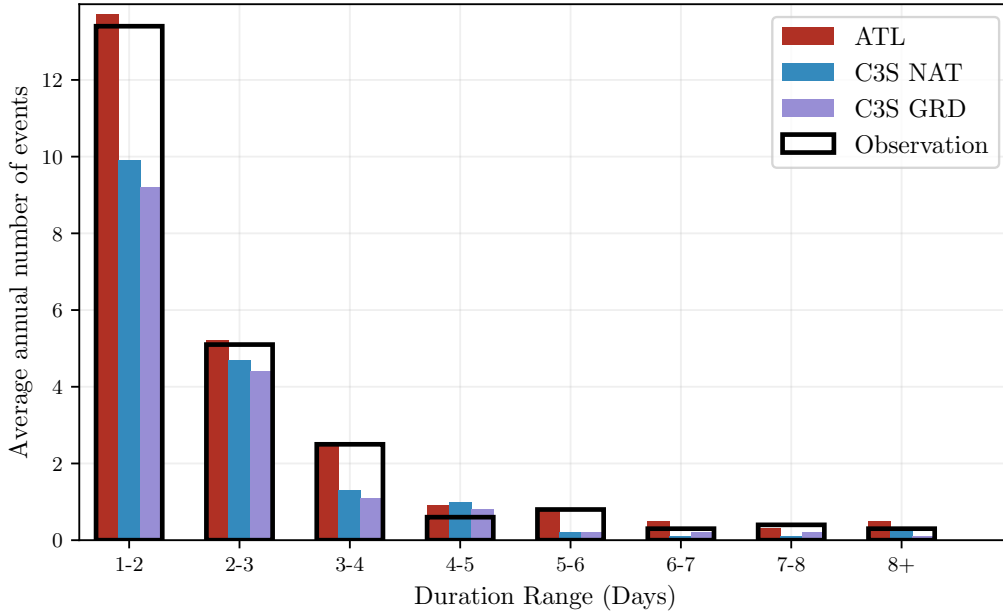


Figure 5: Average annual number of wind drought events for ATL (red), C3S GRD (blue), C3S NAT (purple), and the observed data (black outline). The wind droughts are identified from 2014 to 2023, considering the actual capacity of the system at any given time

294 This verification for wind generation data highlights the importance of  
295 selecting a representative wind turbine power curve for the region being anal-  
296 ysed. The ATL dataset, which uses a representative wind turbine power  
297 curve, is skilled at reproducing wind CF and RES droughts over Ireland. On  
298 the other hand, the power curve used for both C3S GRD and C3S NAT is  
299 not representative for Ireland, as it severely overestimates generation, under-  
300 estimating the occurrence of RES droughts. This highlights a problem with

301 using generalised datasets for analysing RES droughts: biases severely affect  
302 their ability to accurately reproduce RES drought events. The skill scores  
303 for the three datasets (Tab. 2) show only a small difference in their ability to  
304 reproduce the changes in CF, as seen by their similar CC scores. However,  
305 their ability to reproduce the actual CF values is much lower than that of  
306 ATL, with RMSE scores almost four times bigger for the two C3S datasets.  
307 There is a clear bias towards an overestimation of CF, seen in the MBE val-  
308 ues, which leads to the underestimation of RES droughts. This highlights  
309 the need to use regionally verified models to assess RES droughts.

#### 310 4.1.2. Solar PV Energy

311 The Atlite model allows the user to select certain PV panel characteristics.  
312 In this study, the three PV panel types available in the Atlite model were  
313 considered (CSi, CdTe, Kaneka). Following the same methodology as in the  
314 previous section, the three available models were compared using four skill  
315 scores (CC, RMSE, MBE, and the percentage of overlap). Based on the best-  
316 performing metrics, the Beyer PV panel model was selected [25], using the  
317 Kaneka Hybrid panel option. For all solar PV farm locations, the azimuth  
318 angle is fixed at 180°(due south), and the optimal tilt angle option is applied.

319 The solar PV installed capacity available on the spreadsheets from Eir-  
320 Grid represents the Maximum Export Capacity (MEC) and does not ac-  
321 curately reflect the installed solar PV capacity. To enable actual solar PV  
322 generation potential to be modelled correctly, installed capacities were set at  
323 1.4 times the MEC values. This scaling factor was estimated by analysing  
324 proprietary data from individual solar PV farms provided by EirGrid, which  
325 showed that, on average, assuming that the installed capacities of farms ex-  
326 ceed their MEC values by 40% yields the best agreement with the observed  
327 availability.

328 Fig. 6 shows that the three datasets have a similar tendency to overesti-  
329 mate the CF compared to the observed values, especially for high CF values.  
330 The skill scores presented in Table 3 indicate that C3S GRD and C3S NAT  
331 perform better than ATL for solar PV CF, with lower RMSE and MBE,  
332 and higher CC scores. This may be due to the statistical approach taken by  
333 C3SE for the orientation of the PV panels.

334 Fig. 7 shows the number of solar PV drought events during the 2023  
335 validation period across different duration ranges. The figure reveals partial  
336 agreement between the three datasets and the observed data, with consistent  
337 results noticed for duration ranges of 1-2, 3-4, 7-8, and 8+ days. However,

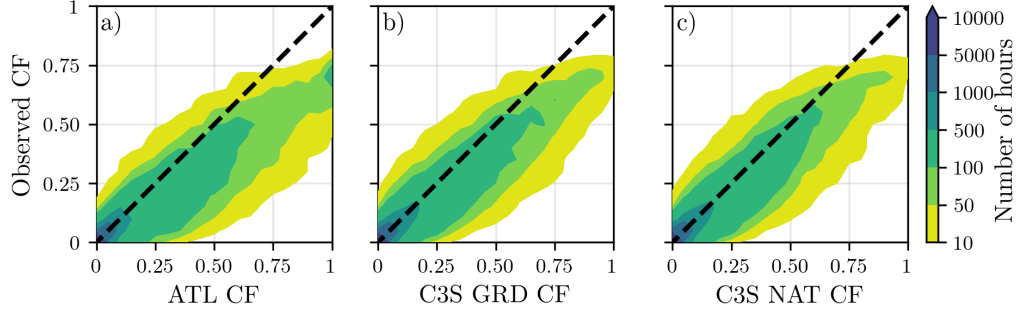


Figure 6: Solar PV CF density plot of the observed (vertical axes) and modelled (horizontal axes) CF series for the a) ATL, b) C3S GRD and c) C3S NAT datasets

	ATL	C3S GRD	C3S NAT
<b>CC</b>	0.921	0.931	0.931
<b>RMSE</b>	0.119	0.090	0.113
<b>MBE</b>	0.046	0.027	0.021

Table 3: Skill scores for solar PV CF for the three datasets compared to observed data

discrepancies appear in the other ranges, where the models diverge from the observed data. The main challenge in validating solar PV data stems from the recent installation of a large share of Ireland’s solar PV capacity, with over 65% of the total solar PV capacity installed in 2023. This results in uncertainties in solar PV generation data and the actual generating capacity in the first few months after each farm is connected. Overall, C3S GRD performs slightly better than the other datasets in reproducing observed solar PV drought events.

#### 4.2. Analysis

In this section, RES droughts are analysed by calculating the frequency and duration of RES drought events, the return periods for different RES drought durations, and the seasonality of RES drought events. Understanding the characteristics and timing of RES drought events enables system operators to optimally plan for reserve capacity requirements, ensuring grid stability and security of supply. Results are presented for the three datasets, allowing their differences on the characterisation of RES droughts to be clearly identified.





Figure 7: Number of solar PV drought events for ATL (red), C3S GRD (blue), and C3S NAT (purple) and the observed data (black outline). The solar PV droughts are identified for 2023, considering the actual capacity of the system at any given time

RES drought events are evaluated under two different scenarios with fixed installed capacities: the 91W-9PV scenario, with 5.9 GW of wind capacity and 0.6 GW of solar PV capacity; and the 57W-43PV scenario, where wind capacity comprises 11.45 GW and solar PV capacity increases to 8.6 GW. Both scenarios were driven by 45 years of ERA5 data. Using the RES drought identification process described in Section 3.5, wind and solar PV droughts are first analysed separately before presenting the results for combined (wind + solar PV) RES droughts under both scenarios.

#### 4.2.1. Annual Number of RES Droughts

The first part of the analysis examines the annual number of RES drought events. When only wind energy is considered (Fig. 8a), the number of RES drought events decreases as the duration range increases, with very few events lasting more than seven days. In contrast, for solar PV energy (Fig. 8b), RES drought frequency declines from one to eight days and then slightly increases for longer durations. This behaviour is attributable to Ireland's high-latitude location, where reduced sunlight in winter (from November to March) leads

371 to consistently low solar PV output.

372 Moreover, the comparison between wind and solar PV results indicates  
373 that the median, first, and third quartiles for solar PV are consistently higher  
374 than or equal to those for wind. This is expected, given that solar PV gener-  
375 ation is inherently lower, zero at night, and limited by the solar cycle. When  
376 wind and solar PV are combined under the 91W-9PV scenario (Fig. 8c), the  
377 results closely mirror those of wind alone, due to the dominance of wind power  
378 in the current energy mix. However, in the 57W-43PV scenario (Fig. 8d), a  
379 marked reduction in RES drought events is observed across all datasets, with  
380 a decrease of the total number of events of 56% for ATL, 52% for C3S GRD,  
381 and 50% for C3S NAT, demonstrating the beneficial effects of a more bal-  
382 anced energy mix.

383 The consistently higher RES drought counts reported by the ATL dataset,  
384 compared to the C3S datasets, underscore the importance of wind turbine  
385 power curve representation when quantifying RES droughts. Whereas the  
386 three datasets agree on the overall effect of balancing the share of wind and  
387 solar PV generation, they differ at a quantitative level, which has crucial  
388 implications for energy planning.

#### 389 4.2.2. Return Periods of RES Drought Duration

390 RES drought events identified over the 45-year period were used to cal-  
391 culate the return periods for different RES drought durations. A return  
392 period is the estimated average time interval between events of a specified  
393 duration (not to be confused with the frequency of their occurrence within a  
394 fixed time frame). Fig. 9 shows the return periods for different RES drought  
395 durations, which can be used to capture the most extreme events affecting  
396 the system. Understanding their return periods is crucial, as extreme yet  
397 rare RES droughts pose the toughest challenge to energy security by placing  
398 significant strain on the conventional backup sources necessary to maintain  
399 security of supply during these events.

400 The duration of wind droughts (Fig. 9a) increases in a log-linear fashion  
401 across the three datasets. The log-linear trend indicates a predictable rela-  
402 tionship between wind drought duration and occurrence, with longer wind  
403 droughts becoming exponentially less likely as duration increases. In the  
404 case of solar PV droughts (Fig. 9b), Atlite behaves differently than the two  
405 C3S datasets. The ATL dataset show a generally log-linear increase. For  
406 C3S GRD and C3S NAT, the duration of PV droughts increases in a log-  
407 linear pattern for events lasting less than 16 days. Beyond this duration,

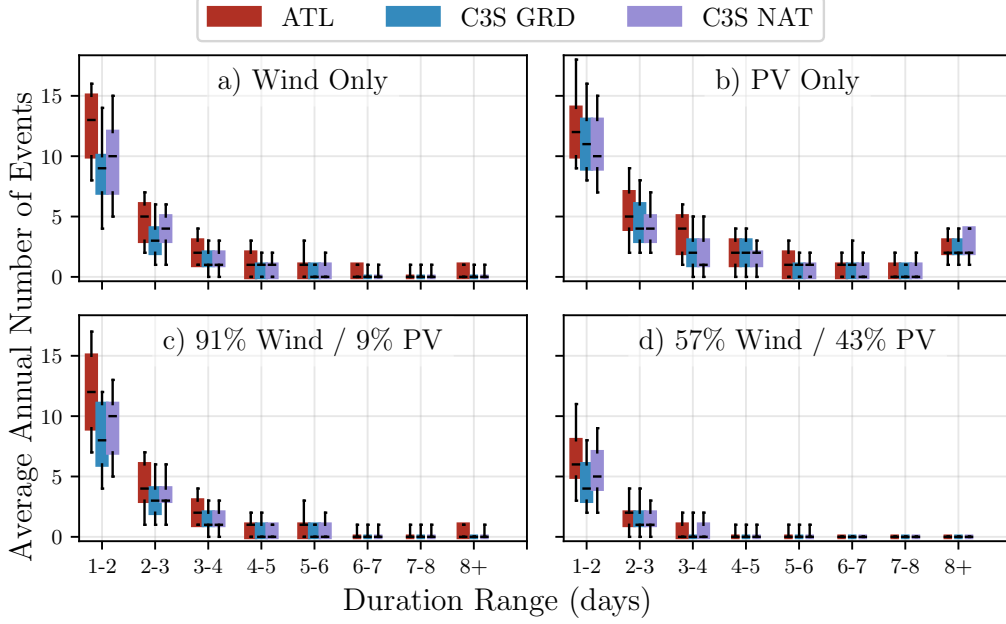


Figure 8: Average annual number of RES droughts (from 1979 to 2023) for a) Wind, b) solar PV, c) 91W-9PV and d) 57W-43PV for ATL (red), C3S GRD (blue), and C3S NAT (purple). The x-axis represents duration ranges in days (lower bound included), while the y-axis indicates the annual number of events. The boxes display the first and third quartiles and the median is marked by a black line. The whiskers indicate the 5th and 95th percentiles

there is a sharp rise in solar PV drought duration for events up to a one-year return period. This sudden increase again reflects the impact of extended periods of low PV generation during winter in Ireland. The difference between the ATL and the C3S results arises from differences in the datasets near the threshold of 0.1 CF. ATL remains slightly above the threshold more frequently during these conditions, leading to shorter, more fragmented RES drought events. In contrast, C3S GRD and C3S NAT tend to fall below the threshold in similar conditions, resulting in longer continuous RES drought periods, especially during winter.

Under the 91W-9PV scenario (Fig. 9c), the combined RES drought return periods mirror those for wind alone, reflecting the dominance of wind in the current energy mix. In contrast, the 57W-43PV scenario (Fig. 9d) shows a dramatic increase in return periods across all durations, suggesting that

421 a more diversified energy mix can substantially mitigate the frequency of  
 422 prolonged RES drought events. For example, the return period for a five-day  
 423 RES drought event (shown by the vertical dashed lines in Fig. 9) extends  
 424 from roughly six months for the 91W-9PV scenario, to four years for the  
 425 57W-43PV scenario in the ATL dataset, and from about fifteen months to  
 426 around five years in the two C3S datasets. Despite the lower wind share in the  
 427 57W-43PV scenario, typically known for its relative stability, the balanced  
 428 share with solar PV leads to extended return periods for RES droughts. This  
 429 result indicates that the complementarity between wind and solar PV plays a  
 430 crucial role in reducing the occurrence of RES drought events in a diversified  
 431 energy portfolio.

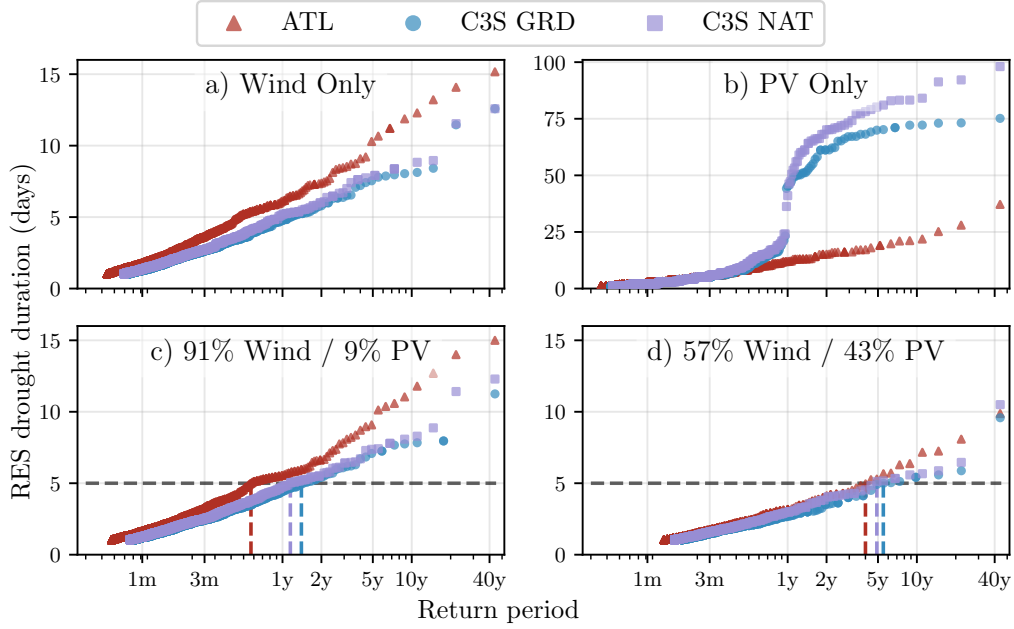


Figure 9: Return periods of the duration of RES droughts (from 1979 to 2023) for a) Wind, b) Solar PV, c) 91W-9PV and d) 57W-43PV for ATL (red triangle), C3S GRD (blue circle), and C3S NAT (purple square). The x-axis represents the return period time in a log-scale and the y-axis indicates the duration of RES drought associated with it. The horizontal dashed line marks the 5-day return period, with coloured vertical dashed marking its return period for each dataset

432 Across Fig. 9a, c, and, d, the return periods in the ATL dataset are con-  
 433 sistently higher than those in the two C3S datasets. For instance, in the

91W-9PV scenario (Fig. 9c), an event with a one-year return period lasts six days in the ATL dataset, compared to only five days in the C3S datasets. This difference underscores the importance of model selection when quantifying RES droughts, as each dataset’s assumptions and parametrisations significantly influence RES droughts duration estimates. Additionally, in all four graphs, the similarity between results from the two C3S datasets suggests that assumptions in the ATL dataset, such as wind turbine power curve selection and PV panel specifications, have a greater impact on RES drought duration estimates than the precise geographic distribution of RES farms when studying the return periods of RES droughts.

The return periods calculated from the three datasets show large differences, in particular for the more extreme events with longer return periods. The C3S datasets produce shorter RES drought durations for these events, which would have the largest impact on the power system. This shows that system planning based on the wrong datasets could yield an underestimation of the duration of extreme RES droughts, potentially leading to shortages linked to undersized reserve capacity.

#### 4.2.3. Seasonal Distribution of RES Droughts

The seasonal analysis of RES droughts is based on the percentage of hours in each month classified as part of a RES drought event. Wind droughts tend to be more frequent during summer, whereas solar PV droughts are more common in winter due to reduced sunlight. By comparing these seasonal patterns across different datasets and energy scenarios, this study examines how model-specific assumptions and variations in capacity mix affect the overall characterisation of RES drought events.

For the wind-only scenario (Fig. 10a), the ATL dataset exhibits a pronounced seasonal pattern, with about 24% of summer hours (June, July, August) identified as RES droughts compared to only 4% in winter (December, January, February). This strong seasonal signal is less evident in the C3S datasets, which suggests that the differences in the underlying wind power curves play a significant role. In ATL, CF near or below the 0.1 threshold occurs at relatively higher wind speeds, resulting in a higher count of RES drought hours during the summer months. In contrast, solar PV droughts (Fig. 10b) display an opposite seasonal trend. Across all datasets, over 60% of winter hours are classified as solar PV droughts, reflecting the naturally low solar irradiance in Ireland during winter.

ATL tends to record a slightly higher percentage of RES drought hours

471 for wind and a marginally lower percentage for solar PV relative to the C3S  
472 datasets. These differences highlight how dataset-specific assumptions, such  
473 as the treatment of wind turbine power curves and PV panel characteristics,  
474 significantly influences the apparent seasonal dynamics of RES droughts.

475 The 91W-9PV scenario (Fig. 10c) shows patterns comparable to the ones  
476 for wind droughts (Fig. 10a). However, in the 91W/9PV scenario, the number  
477 of hours classified as RES droughts in summer decreases slightly compared to  
478 the wind-only scenario. This reduction can be explained by the contribution  
479 of solar PV generation during the summer months in the 91W-9PV scenario,  
480 even though it constitutes only 11% of total capacity. Since the number of  
481 RES drought hours for solar PV in summer is near zero, this small contri-  
482 bution has a noticeable impact on reducing overall RES drought hours. In  
483 the 57W-43PV scenario (Fig. 10d), all three datasets show a reduction in  
484 monthly RES drought frequency. Annual reductions in median RES drought  
485 frequency are observed across the datasets, dropping from 14% to 5% for  
486 ATL, from 8% to 3% for C3S GRD, and from 9% to 4% for C3S NAT. The  
487 balanced mix of wind and solar PV power in this scenario reduces the sea-  
488 sonal signal overall and significantly decreases the percentage of RES drought  
489 hours in the summer.

490 The seasonal variations of RES droughts observed in this study have im-  
491 portant implications for energy planning. Energy demand peaks in winter  
492 for Northern European countries, making the seasonality of RES droughts  
493 critical for the sizing of reserve capacity. Our results show that selecting  
494 the wrong dataset could severely underestimate RES droughts during winter  
495 months, thereby affecting the reliability of the energy system during critical  
496 periods. Additionally, the integration of large shares of solar PV in the system  
497 leads to a generalised reduction of RES droughts, yet winter months present  
498 a slight increase. The natural limitations of solar PV lead to inevitably  
499 higher reserve capacity needs during winter months as reliance on RES in-  
500 creases. These types of insights are essential to develop targeted strategies  
501 that enhance grid resilience and ensure a stable energy supply throughout  
502 the year.

## 503 5. Conclusions

504 The two questions presented and answered in this study are: XXX?;  
505 YYY? Three different datasets were compared over a 45-year period: one  
506 created using a regionally validated model and two derived from a generic

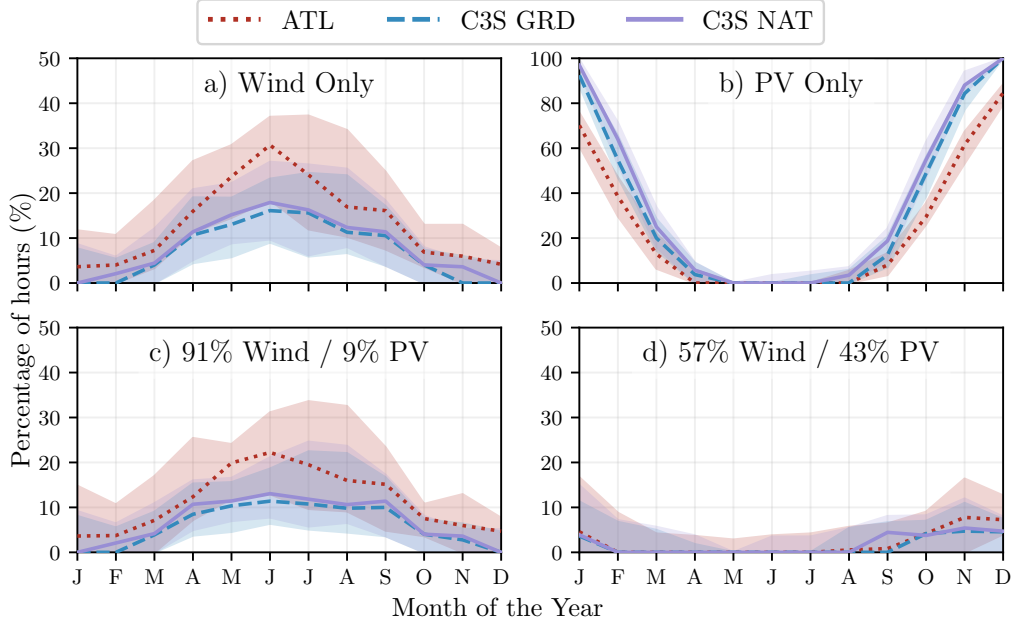


Figure 10: Percentage of hours in a month which are part of a RES drought (from 1979 to 2023) for a) Wind, b) Solar PV, c) 91W-9PV and d) 57W-43PV for ATL (red dotted), C3S GRD (blue dashed), and C3S NAT (purple solid). The x-axis represents the month of the year, and the y-axis indicates the percentage of hours. Lines correspond to the median values and the area between the first and third quartiles is shaded. Note the different y-axis scale for b).

dataset for Europe, C3S-Energy. The two datasets derived from C3S-Energy present different approaches, with one using large-scale aggregated information only, and the other one including the locations of farms as well. The regionally validated model considered the locations of farms as well as tailored wind and solar PV models selected to best represent the actual generation in Ireland.

Our results show the limitations in the quantification of RES droughts present in datasets that have not undergone regional validation. The three datasets used in this study are able to capture overall trends in RES drought occurrence such as the seasonal cycle or the effect of increasing the share of solar PV. However, significant differences in the quantitative values, particularly the extremes, emerge when using non-validated datasets for the study of RES droughts. This finding highlights that using a non-validated

dataset can lead to undersized reserve capacity, with the associated negative consequences for grid stability and security of supply.

This study has also revealed that differences in the wind turbine power curves and solar PV panel models have a stronger influence on the estimation of RES droughts than the consideration of RES farm locations. The two datasets derived from C3S-Energy consistently underestimated the number of wind drought events and the frequency of extremes when compared to the regionally validated dataset with a specifically selected wind turbine power curve. This suggests that a meticulous selection of the wind turbine power curve to match observed data is crucial for accurately quantifying RES drought risks, thereby supporting more effective energy system planning.

Finally, the effect of the integration of solar PV in a wind-dominated system on RES droughts has been explored in a real-case setting based on Ireland. Our analysis has demonstrated that transitioning to a system with similar amounts of wind and solar PV reduces the frequency, duration, and seasonal variability of RES drought events. This improvement is attributed to the complementary nature of wind and solar PV generation, as solar PV typically peaks in summer while wind generation is more consistent in winter. However, this integration is unable to counter the critical winter RES droughts, which coincide with the strongest electricity demand in Northern European countries like Ireland. Still, a more diversified renewable energy mix mitigates extreme RES drought conditions and enhances overall system resilience.

The results presented in this study have four main limitations. First, the presented study uses a fixed threshold to define RES drought events, but other methods could yield different results, even though the main takeaways would be expected to be the same. Second, the definition of RES droughts based on generation does not consider the important role of demand, which could be of interest to system operators. Third, the availability of solar PV data is limited to a relatively short time period, as recent expansions in installed capacity have significantly changed the generation landscape. Lastly, the source for weather data is ERA5, which is among the best reanalysis datasets for renewable energy applications, but still comes in a limited spatial resolution, an issue that can be addressed once higher resolution datasets become available.

Future work is planned to extend the current analysis. First, climate projection data will be integrated with different energy scenarios, incorporating the addition of offshore wind, to better understand how climate change might



558 affect RES droughts. Second, expanding the geographic domain of the study  
559 to include the rest of Europe would provide a more comprehensive under-  
560 standing of RES droughts in an interconnected electricity grid. This would  
561 require extensive verification across other European countries, making it a  
562 more complex but highly relevant challenge.

## 563 Data Availability

564 The ERA5 data can be obtained from the Climate Data Store (<https://doi.org/10.24381/cds.adbb2d47>). The C3SE dataset is also available  
565 from the Climate Data Store (<https://doi.org/10.24381/cds.4bd77450>).  
566 Information on wind and solar PV farms in Ireland can be obtained from  
567 the EirGrid website (<https://www.eirgrid.ie/grid/system-and-renewable-data-reports>). The Atlite model used in this study is open-source  
568 and can be found on GitHub (<https://github.com/pypsa/atlite>). The  
569 data and code required to reproduce the analysis in this article will be made  
570 available upon acceptance of the manuscript in a public GitHub repository.  
571  
572

## 573 Acknowledgments

574 The research conducted in this publication was funded by Science Foun-  
575 dation Ireland and co-funding partners under grant number 21/SPP/3756  
576 through the NexSys Strategic Partnership Programme.

## 577 References

- 578 [1] EuroStat, Renewable Energy Statistics, 2023. URL: [https://ec.europa.eu/eurostat/statistics-explained/index.php?title=Renewable\\_energy\\_statistics](https://ec.europa.eu/eurostat/statistics-explained/index.php?title=Renewable_energy_statistics), Accessed: 2024-11-06.  
579  
580
- 581 [2] H. C. Bloomfield, D. J. Brayshaw, L. C. Shaffrey, P. J. Coker, H. E. Thornton, Quantifying the increasing sensitivity of power systems to  
582 climate variability, *Environmental Research Letters* 11 (2016) 124025.  
583 doi:10.1088/1748-9326/11/12/124025.  
584
- 585 [3] H. C. Bloomfield, D. J. Brayshaw, A. Troccoli, C. M. Goodess, M. De Felice, L. Dubus, P. E. Bett, Y.-M. Saint-Drenan, Quantifying the  
586 sensitivity of european power systems to energy scenarios and climate change projections, *Renewable Energy* 164 (2021) 1062–1075.  
587 doi:10.1016/j.renene.2020.09.125.  
588  
589

- [4] F. Kaspar, M. Borsche, U. Pfeifroth, J. Trentmann, J. Drücke, P. Becker, A climatological assessment of balancing effects and shortfall risks of photovoltaics and wind energy in germany and europe, *Advances in Science and Research* 16 (2019) 119–128. doi:10.5194/asr-16-119-2019.
- [5] F. Mockert, C. M. Grams, T. Brown, F. Neumann, Meteorological conditions during periods of low wind speed and insolation in Germany: The role of weather regimes, *Meteorological Applications* 30 (2023) e2141. doi:10.1002/met.2141.
- [6] M. Ohba, Y. Kanno, D. Nohara, Climatology of dark doldrums in japan, *Renewable and Sustainable Energy Reviews* 155 (2022) 111927. doi:10.1016/j.rser.2021.111927.
- [7] M. J. Mayer, B. Biró, B. Szücs, A. Aszódi, Probabilistic modeling of future electricity systems with high renewable energy penetration using machine learning, *Applied Energy* 336 (2023) 120801. doi:10.1016/j.apenergy.2023.120801.
- [8] D. Raynaud, B. Hingray, B. François, J. Creutin, Energy droughts from variable renewable energy sources in European climates, *Renewable Energy* 125 (2018) 578–589. doi:https://doi.org/10.1016/j.renene.2018.02.130.
- [9] A. Gangopadhyay, A. K. Seshadri, N. J. Sparks, R. Toumi, The role of wind-solar hybrid plants in mitigating renewable energy-droughts, *Renewable Energy* 194 (2022) 926–937. doi:10.1016/j.renene.2022.05.122.
- [10] J. Kapica, J. Jurasz, F. A. Canales, H. Bloomfield, M. Guezgouz, M. De Felice, Z. Kobus, The potential impact of climate change on european renewable energy droughts, *Renewable and Sustainable Energy Reviews* 189 (2024) 114011. doi:10.1016/j.rser.2023.114011.
- [11] K. Z. Rinaldi, J. A. Dowling, T. H. Ruggles, K. Caldeira, N. S. Lewis, Wind and Solar Resource Droughts in California Highlight the Benefits of Long-Term Storage and Integration with the Western Interconnect, *Environmental Science and Technology* 55 (2021) 6214–6226. doi:10.1021/acs.est.0c07848.

- [12] P. T. Brown, D. J. Farnham, K. Caldeira, Meteorology and climatology of historical weekly wind and solar power resource droughts over western North America in ERA5, *SN Applied Sciences* 3 (2021) 814. doi:10.1007/s42452-021-04794-z.
- [13] S. Allen, N. Otero, Standardised indices to monitor energy droughts, *Renewable Energy* 217 (2023) 119206. doi:10.1016/j.renene.2023.119206.
- [14] C. Bracken, N. Voisin, C. D. Burleyson, A. M. Campbell, Z. J. Hou, D. Broman, Standardized benchmark of historical compound wind and solar energy droughts across the Continental United States, *Renewable Energy* 220 (2024) 119550. doi:https://doi.org/10.1016/j.renene.2023.119550.
- [15] H. Lei, P. Liu, Q. Cheng, H. Xu, W. Liu, Y. Zheng, X. Chen, Y. Zhou, Frequency, duration, severity of energy drought and its propagation in hydro-wind-photovoltaic complementary systems, *Renewable Energy* (2024) 120845. doi:10.1016/j.renene.2024.120845, 2.
- [16] H. Hersbach, B. Bell, P. Berrisford, S. Hirahara, A. Horányi, J. Muñoz-Sabater, J. Nicolas, C. Peubey, R. Radu, D. Schepers, et al., The ERA5 global reanalysis, *Quarterly Journal of the Royal Meteorological Society* 146 (2020) 1999–2049. doi:10.1002/qj.3803.
- [17] L. Dubus, Y. Saint-Drenan, A. Troccoli, M. De Felice, Y. Moreau, L. Ho-Tran, C. Goodess, R. Amaro E Silva, L. Sanger, C3S Energy: A climate service for the provision of power supply and demand indicators for Europe based on the ERA5 reanalysis and ENTSO-E data, *Meteorological Applications* 30 (2023) e2145. doi:10.1002/met.2145.
- [18] F. Hofmann, J. Hampp, F. Neumann, T. Brown, J. Hörsch, Atlite: a lightweight Python package for calculating renewable power potentials and time series, *Journal of Open Source Software* 6 (2021) 3294. doi:10.21105/joss.03294.
- [19] A. Kies, B. U. Schyska, M. Bilousova, O. El Sayed, J. Jurasz, H. Stoecker, Critical review of renewable generation datasets and their implications for european power system models, *Renewable and Sustainable Energy Reviews* 152 (2021) 111614. doi:10.1016/j.rser.2021.111614.

- 657 [20] EirGrid & SONI, System and Renewable Data Reports, 2023. URL:  
658 [https://www.eirgrid.ie/grid/system-and-renewable-data-rep](https://www.eirgrid.ie/grid/system-and-renewable-data-reports)  
659 [orts](https://www.eirgrid.ie/grid/system-and-renewable-data-reports), Accessed: 2024-11-06.
- 660 [21] Y.-M. Saint-Drenan, L. Wald, T. Ranchin, L. Dubus, A. Troccoli, An  
661 approach for the estimation of the aggregated photovoltaic power gener-  
662 ated in several European countries from meteorological data, *Advances*  
663 *in Science and Research* 15 (2018) 51–62. doi:10.5194/asr-15-51-201  
664 8.
- 665 [22] I. Staffell, S. Pfenninger, Using bias-corrected reanalysis to simulate  
666 current and future wind power output, *Energy* 114 (2016) 1224–1239.  
667 doi:10.1016/j.energy.2016.08.068.
- 668 [23] Government of Ireland, Climate Action Plan 2024, Technical Report 3,  
669 Department of the Environment, Climate and Communications, 2023.  
670 URL: [https://www.gov.ie/pdf/?file=https://assets.gov.ie/](https://www.gov.ie/pdf/?file=https://assets.gov.ie/284675/70922dc5-1480-4c2e-830e-295afd0b5356.pdf)  
671 [284675/70922dc5-1480-4c2e-830e-295afd0b5356.pdf](https://www.gov.ie/pdf/?file=https://assets.gov.ie/284675/70922dc5-1480-4c2e-830e-295afd0b5356.pdf), Accessed:  
672 2024-11-06.
- 673 [24] Sustainable Energy Authority Ireland, National Energy Projections  
674 2024, Technical Report, Sustainability Energy Authority of Ireland,  
675 2024. URL: [https://www.seai.ie/news-and-events/news/energ](https://www.seai.ie/news-and-events/news/energy-projections-report)  
676 [y-projections-report](https://www.seai.ie/news-and-events/news/energy-projections-report), Accessed: 2024-11-06.
- 677 [25] H. G. Beyer, G. Heilscher, S. Bofinger, A robust model for the mpp  
678 performance of different types of pv-modules applied for the performance  
679 check of grid connected systems, *Eurosun* (2004) 8.